Long, S.P., 2023, Westward underthrusting of thick North American crust: The dominant thickening process that built the Cordilleran orogenic plateau: Geology, https://doi.org/10.1130/G51339.1

Supplemental Material

Includes a figure with detailed versions of all seven cross sections, a summary of rock units on each cross section, and supporting data for cross section reconstructions, shortening and extension calculations, stratigraphic thicknesses, and measured thickening and thinning components.

Data Repository for: Westward underthrusting of thick North American crust: the dominant thickening process that built the Cordilleran orogenic plateau

Figure S1 (see accompanying oversized jpeg): Deformed and restored versions of seven balanced cross sections through the Sevier fold-thrust belt, ordered from north to south (see Figure 1 in the main text for the locations of their lines of section). All cross sections are oriented with foreland-ward (i.e., toward the northeast, east, or southeast) toward the right-hand side. All cross sections are shown at the same scale (with no vertical exaggeration) and with the same unit color scheme, and all are restored so that the base of the Cretaceous sedimentary section is at a reference crustal thickness of zero. Transparent areas on the restored cross sections that lie above the restored positions of the modern surface represent eroded rock.

Discussion S1: Summary of rock units on each cross section

Cross sections 1 and 2 (Price, 1981; his Figure 2): Mesoproterozoic metasedimentary rocks shown in gray include the 'Lower Belt-Purcell' and 'Upper and Middle Belt-Purcell' units (note: a guide to the rock units used in Price, 1981, is shown on his Figure 1). Neoproterozoic-Early Cambrian sedimentary rocks shown in brown include the 'Windermere' and 'Eo-Cambrian Quartz Sandstone' units. Middle Cambrian-Devonian sedimentary rocks shown in light blue include the 'Lower Paleozoic' units, which are undivided in the Eugeoclinal domain and are divided into a shale unit and a carbonate unit in the Miogeoclinal-Platform domain. Mississippian-Permian sedimentary rocks shown in dark blue include the 'Upper Paleozoic' units, which are shown with different fill symbols in the Eugeoclinal domain and Miogeoclinal-Platform domain. Triassic-Early Jurassic sedimentary rocks shown in blue-green include the 'Triassic-Jurassic' units, which are shown with different fill symbols in the Eugeoclinal Domain and the Miogeoclinal-Platform domain. Cretaceous sedimentary rocks shown in dark green include the undifferentiated 'Upper Jurassic-Paleocene Foredeep Clastic Rocks' unit (see footnote 1 on Figure S1 for further discussion). Oligocene-Quaternary sedimentary rocks and sediment shown in yellow (cross section 2 only) include the 'Tertiary-Recent' unit. Granitic rocks shown in red include the 'Upper Jurassic-Paleocene Granitic Rocks' unit.

Cross section 3 (Fuentes et al., 2012; their Figure 7): Mesoproterozoic metasedimentary rocks shown in gray include the following formations (in ascending stratigraphic order) (units are listed on Figure 6 in Fuentes et al., 2012; additional details on stratigraphy are given in their Figures 3 and 4): Lower Belt Supergroup Rocks (the Prichard Formation), the Greyson Formation, Spokane Formation, Empire Formation, Helena Formation, Snowslip Formation, Shepard Formation, Mount Shields Formation, Bonner Quartzite, McNamara Formation, and Garnet Range Formation. Middle Cambrian-Devonian sedimentary rocks shown in light blue include their Middle-Upper Cambrian (undivided) unit and their Middle-Upper Devonian (undivided) unit. Mississippian-Permian sedimentary rocks shown in dark blue include their Mississippian (undivided) unit. Middle-Late Jurassic sedimentary rocks shown in light green include their undivided Ellis Group and Morrison Formation unit. Cretaceous sedimentary rocks shown in dark green include (in ascending order) the Kootenai Formation, Blackleaf Formation, Marias River Shale, Telegraph Creek and Virgelle Formations, Two Medicine Formation, Horsethief and Bearpaw Formations, and Saint Mary River Formation. Oligocene-Quaternary sedimentary rocks and sediment shown in yellow include their Cenozoic (undivided) unit.

Cross section 4 (Coogan, 1992; his Plate 2c): Precambrian crystalline basement shown in pink includes unit pCx (Archean Crystalline Rocks). Neoproterozoic-Early Cambrian sedimentary rocks shown in brown that restore in the footwall of the Meade thrust include units Ct (Tintic Quartzite) and Cf (Flathead Quartzite), which are shown as laterally equivalent. Neoproterozoic-Early Cambrian sedimentary rocks shown in brown in the hanging walls of the Meade, Willard, and Paris thrusts include (in ascending order) units pCp (Pocatello Formation), pCb (lower Brigham Group, consisting of the Papoose Creek Formation, Caddy Canyon Formation, and Inkom Formation), and pCCb (upper Brigham Group, consisting of the Mutual Formation, Camelback Mountain Quartzite, and Sedgewick Peak Quartzite). Middle Cambrian-Devonian sedimentary rocks shown in light blue that restore foreland-ward of the Meade thrust include units Cg (Gros Ventre Formation-Gallatin Limestone), Ob (Bighorn Dolomite), and Dd (Darby Formation). Middle Cambrian-Devonian sedimentary rocks shown in light blue in the hanging walls of the Meade, Willard, and Paris thrusts include (in ascending order) units Cul (Langston Formation-Ute Formation), Cbl (Backsmith Dolomite), Cbo (Bloomington Formation), Cn (Nounan Formation), Csc (Saint Charles Formation), Osg (Garden City Limestone-Swan Peak Quartzite), Sl (Laketown Dolomite), and Dbhw (Water Canyon Formation-Hyrum Dolomite-Beirdneau Formation). Mississippian-Permian sedimentary rocks shown in dark blue include units Mm (Madison Group) and PIPM (Amsden Formation-Wells Formation-Phosphoria Formation). Triassic-Early Jurassic sedimentary rocks shown in blue-green include units Trwd (Dinwoody Formation-Woodside Formation), Trt (Thaynes Formation), Tra (Ankareh Formation) and Jn (Nugget Sandstone). Middle-Late Jurassic sedimentary rocks shown in light green include units Jtc (Twin Creek Limestone; locally subdivided into members) and Jsp (Preuss Redbeds-Stump Sandstone). Cretaceous sedimentary rocks shown in dark green that restore in the footwall of the Absaroka thrust include units Kg (Gannett Group), Kb (Bear River Formation), Ka (Aspen Formation), Kf (Frontier Formation), Kh (Hilliard Formation), Ka (Adaville Formation), and Khb (Hoback Formation). Cretaceous sedimentary rocks shown in dark green that restore hinterland-ward of the Absaroka thrust include units Kg (Gannett Group), Kst (Smiths Formation-Thomas Fork Formation), Kc (Cokeville Formation), Kq (Quealy Formation), and Ksj (Sage Junction Formation). Paleocene-early Eocene rocks shown in orange include units Tw (Wasatch Formation; locally divided into members), Tgr (Green River Formation), and Tlm (Lookout Mountain Conglomerate). Oligocene-Quaternary sedimentary rocks and sediment shown in yellow include units Tsl (Salt Lake Formation), QT, and Q.

Cross section 5 (Coogan, 1992; his Plate 2a): Precambrian crystalline basement shown in pink includes unit pCf (Farmington Canyon Complex). Neoproterozoic-Early Cambrian sedimentary rocks shown in brown that restore in the footwall of the Willard thrust include units Ct (Tintic Quartzite) and Cf (Flathead Quartzite), which are shown as laterally equivalent. Neoproterozoic-Early Cambrian sedimentary rocks shown in brown in the hanging wall of the Willard thrust include (in ascending order) units pCmp (Perry Canyon Formation and Maple Canyon Formation), pCk (Kelly Canyon Formation), pCc (Caddy Canyon Formation), pCi (Inkom Formation), pCm (Mutual Formation), pCb (Browns Hole Formation) (units pCc, pCi, pCm, and pCb are shown as unit pCb (Brigham Group, undifferentiated) in hinterland portions of the Willard thrust sheet), and units pC-Cm (Prospect Mountain Quartzite) and pC-Cg (Geertzen

Canyon Quartzite; locally divided into lower and upper subunits), which are shown as laterally equivalent. Middle Cambrian-Devonian sedimentary rocks shown in light blue that lie in the footwall of the Willard thrust include units Cg (Gros Ventre Formation-Gallatin Limestone), Ob (Bighorn Dolomite), and Dd (Darby Formation). Middle Cambrian-Devonian sedimentary rocks shown in light blue that lie in the hanging wall of the Willard thrust include (in ascending order) units Cbu (Ute Formation-Backsmith Dolomite), Cbo (Bloomington Formation) (units Cbu and Cbo are shown as laterally equivalent to units Cl (lower Cambrian, undifferentiated) and Cm (Marjum Formation) that are shown in hinterland positions in the Willard thrust hanging wall), Cn (Nounan Formation), Csc (Saint Charles Formation), O-S (locally shown as 'O') (Ordovician-Silurian, undifferentiated), and D (Devonian, undifferentiated). Mississippian-Permian sedimentary rocks shown in dark blue include units Mm (Madison Group) (locally shown as 'M' (Mississippian, undifferentiated)) and PIPM (Amsden Formation-Wells Formation-Phosphoria Formation). Triassic-Early Jurassic sedimentary rocks shown in blue-green include units Trwd (Dinwoody Formation-Woodside Formation), Trt (Thaynes Formation), Tra (Ankareh Formation) and Jn (Nugget Sandstone). Middle-Late Jurassic sedimentary rocks shown in light green include units Jtc (Twin Creek Limestone), Jsp (Preuss Redbeds-Stump Sandstone), and JKg (Gannett Group). Cretaceous sedimentary rocks shown in dark green include units Kb (Bear River Formation), Ka (Aspen Formation), Kf (Frontier Formation), Kh (Hilliard Formation), Ka (Adaville Formation), and Ke (Cretaceous portion of Evanston Formation). Paleocene-early Eocene rocks shown in orange include units TKe (Cretaceous-Paleogene portion of Evanston Formation) and Tw (Wasatch Formation). Oligocene-Quaternary sedimentary rocks and sediment shown in yellow include unit Tf (Fowkes Formation), the 'Oligocene-Eocene?' unit, the 'Miocene' unit, and the 'Holocene' unit.

Cross section 6 (DeCelles and Coogan, 2006; their Figure 8F (deformed), which is a version of their Figure 3 that is restored for Cenozoic extension, and their Figure 8A (restored)): Precambrian crystalline basement shown in pink includes their 'Precambrian crystalline basement (~1.7 Ga)' unit (note: a detailed list of stratigraphic units is shown on Figure 4 of DeCelles and Coogan, 2006). Neoproterozoic-Early Cambrian sedimentary rocks shown in brown include their 'Proterozoic-lower Cambrian sedimentary rocks (mainly quartzite)' unit (consisting of the Pocatello Formation, Caddy Canyon Formation, Inkom Formation, Mutual Formation, and Tintic Formation). Middle Cambrian-Devonian sedimentary rocks shown in light blue include their 'Cambrian-Devonian sedimentary rocks (mainly carbonates)' unit (consisting of the Pioche Formation, Undifferentiated Cambrian limestone and shale, the Pogonip Group, Simonson Dolomite, Guilmette Formation, and Cove Fort Quartzite). Mississippian-Permian sedimentary rocks shown in dark blue include their 'Carboniferous-Permian sedimentary rocks' unit. Triassic-Early Jurassic sedimentary rocks shown in blue-green include their 'Triassic-Middle Jurassic sedimentary rocks' unit. Middle-Late Jurassic sedimentary rocks shown in light green include their 'Middle-Upper Jurassic synorogenic sedimentary rocks' unit. Cretaceous sedimentary rocks shown in dark green include their 'Cretaceous synorogenic sedimentary rocks' unit.

Cross section 7 (Giallorenzo et al., 2018; their Figure 3 (deformed); restored cross section is from this study (see Footnote 17 on Figure S1 for additional details on restoration)). Neoproterozoic-Early Cambrian sedimentary rocks shown in brown in the footwall of the Keystone thrust include their unit Cq (Cambrian lower). Neoproterozoic-Early Cambrian sedimentary rocks shown in brown in the hanging wall of the Lee Canyon thrust and Wheeler Pass thrust include (in ascending order) their units Zpn (Pahrump Group plus Noonday Formation), Zj (Johnnie Formation), Zs (Stirling Quartzite), and ZCw (Wood Canyon-Carrara Formations). Middle Cambrian-Devonian sedimentary rocks shown in light blue in the footwall of the Keystone thrust include their units Cu (Cambrian upper) and D (Devonian strata). Middle Cambrian-Devonian sedimentary rocks shown in light blue in the hanging walls of the Keystone, Lee Canyon, and Wheeler Pass thrusts include their units Cb (Bonanza King Formation), Cn (Cambrian upper strata), O (Ordovician strata), and the bottom half of their unit MD (Devonian-Mississippian strata). Mississippian-Permian sedimentary rocks shown in dark blue in the footwall of the Keystone thrust include their units PM (Pennsylvanian-Mississippian strata) and P (Permian strata). Mississippian-Permian sedimentary rocks shown in dark blue in the hanging walls of the Keystone, Lee Canyon, and Wheeler Pass thrusts include the top half of their unit MD (Devonian-Mississippian strata) and their unit Pb (Bird Spring Formation). Triassic-Early Jurassic sedimentary rocks shown in blue-green are only exposed in the footwall of the Keystone thrust, and include their units Tr (Triassic strata) and J (Jurassic strata).

Discussion S2: Methods of reconstruction and calculation of shortening and extension

The geometries shown on the deformed cross sections on Figure S1 are directly from the cited source publications, with the exception of cross sections 1 and 2, in which I interpreted geometries for portions of hinterland thrust sheets that were left blank on Price (1981) (see Footnotes 2 and 6 on Figure S1 for additional details). The geometries shown on the restored cross sections on Figure S1 are directly from the cited source publications for cross sections 4-6. However, I projected the restored sections for cross sections 1-3 further westward than those shown in Price (1981) and Fuentes et al. (2012) by using line-length balancing to restore several hinterland thrust sheets (see Footnotes 4, 8, and 9 on Figure S1 for additional details). For cross sections 1 and 2, I did not attempt to restore the complexly folded rocks exposed in the Kootenay Arc (see Footnotes 3 and 7 on Figure S1). Additionally, I drafted the entire restored section for cross section 7, using geometric constraints from the deformed cross section of Giallorenzo et al. (2018) (see Footnote 17 on Figure S1). In all cases, I made drafting decisions that attempted to minimize displacement on thrust faults, and thus to minimize the amount of shortening necessary to produce the final geometry.

To estimate the approximate level of the surface at the timing of initiation of shortening in the Sevier fold-thrust belt, the top of the Middle-Late Jurassic sedimentary unit (or the top of the Triassic-Early Jurassic sedimentary unit when no Middle-Late Jurassic sedimentary rocks are present) is shown at a reference crustal thickness of zero on the restored versions of all seven cross sections (Figure S1; also shown on Figures 2 and 4 in the main text). Middle-Late Jurassic rocks have been interpreted by several researchers to represent early synorogenic sedimentary rocks that were deposited in a distal foreland basin setting (forebulge and backbulge depocenters), perhaps as much as ~200-600 km foreland-ward of the growing Cordilleran orogenic wedge to the west (e.g., DeCelles, 2004; DeCelles and Coogan, 2006; Fuentes et al., 2012). Therefore, the Middle-Late Jurassic section was likely mostly or completely deposited prior to the eastward migration of the thrust front into the area shown on the cross sections. Therefore, I used the top of the Middle-Late Jurassic section (equivalent to the base of the Cretaceous section) to approximate a sub-horizontal datum that represents the surface level at the timing of initiation of shortening in the Sevier fold-thrust belt.

For pre-Cretaceous rock units that did not have complete thicknesses exposed in the hinterland portions of the cross sections, these units were projected to the western edge of the restored sections using their westernmost exposed complete thicknesses. This applies primarily to rock units between Mississippian and Jurassic in age, particularly on cross sections 1, 2, 5, and 7. Based on the general westward thickening of most pre-Cretaceous rock units, this method likely resulted in conservative cumulative thickness estimates moving westward.

On all of the deformed cross sections (with the exception of cross section 6, for which I show a version that is already restored for post-orogenic extension; see Footnote 14 on Figure S1), I calculated cumulative post-orogenic extension by measuring the extension magnitude accommodated on individual normal faults. This was accomplished by measuring the horizontal distance (in km) between the intersections of the hanging wall and footwall cutoffs of a matching stratigraphic contact with the normal fault (in several cases, stratigraphic contacts from un-lumped stratigraphic units on the source cross sections were used), which are shown as orange bars and numbers above individual normal faults on each deformed cross section on Figure S1. The extension on all individual normal faults along the length of the deformed cross section was then added to yield the total extension magnitude.

For each cross section, I assigned a point on the western edge of the restored cross section as a deformation marker, and I matched its location at a point on the western edge of the deformed cross section (these reference deformation markers are shown as blue circles on Figure S1). I measured the restored length of each cross section (listed in blue text above each restored cross section on Figure S1) by measuring the total horizontal distance between the thrust front (see Footnotes 5 and 15 on Figure S1 for explanation of how the thrust front was determined on cross sections 2 and 6, which lack emergent frontal thrust faults) and the reference deformation marker. I measured the modern (i.e., post-extensional) length of each deformed cross section by measuring the total horizontal distance between the thrust front and the reference deformation marker. I then subtracted the total extension measured along the length of the deformed cross section from the modern length to calculate the pre-extensional length (both are listed in orange text above each deformed cross section on Figure S1). Finally, I calculated shortening for each cross section by subtracting the pre-extensional length from the restored length (listed in blue text to the left of each deformed cross section on Figure S1). Percent shortening was calculated by dividing shortening by the restored length (Table S1).

For each cross section, I measured the distances along the restored section between the thrust front and the point at which the cumulative thickness of pre-Cretaceous sedimentary rocks above the basal thrust décollement attained values of 2.5 km, 5 km, 7.5 km, 10 km, and so forth (supporting data shown in Table S2). I also measured the total thickness of pre-Cretaceous sedimentary rocks at the western edge of each restored cross section. For cross sections 4-6, I projected the minimum thicknesses of Neoproterozoic-Early Cambrian rocks that lie above the basal dècollement that have been measured in proximal ranges that lie to the west of the restored cross sections, in order to estimate the minimum depth to dècollement (see Footnotes 11, 13, and 16 on Figure S1). For cross section 4, this included a 5.4 km minimum thickness (Yonkee et al., 2014) projected from the Bannock Range ~60 km to the north and ~15 km to the west of the western edge of the restored section (Figure S1, Footnote 11). For cross section 5, this included a 7.3 km minimum thickness (Christie-Blick, 1997) projected from the Sheeprock Mountains ~140 km to the south and ~10 km to the west of the western edge of the restored section (Figure S1, Footnote 13). For cross section 6, this included a 7.3 km minimum thickness (Rodgers, 1987) projected from the Deep Creek Range ~60 km to the north and ~35 km to the west of the western edge of the restored section (Figure S1, Footnote 16).

In order to plot the thicknesses of pre-Cretaceous sedimentary rocks on the contour map on Figure 3A in the main text, which shows present-day dimensions, it was necessary to account for the overprinting effects of Cenozoic extension. To achieve this, I measured incremental extension magnitudes between each of the measured points along the restored sections at which pre-Cretaceous sedimentary rocks reached 2.5 km thickness increments (supporting data shown in Table S2). Along the length of the deformed cross sections, I utilized the extension magnitudes that I measured from contacts offset across normal faults (described above and listed on Figure S1) to measure incremental extension magnitudes. For the areas that lie to the west of the deformed sections, I utilized published regional reconstructions of extension to calculate incremental extension values for cross sections 4-7 (I did not incorporate any extension estimates for cross sections 1-3, as I am not aware of any regional-scale studies that have estimated extension in these regions). I added the incremental extension values to calculate cumulative extension. I then added these cumulative extension values to the distances along the restored sections at which pre-Cretaceous sedimentary rocks reached 2.5 km thickness increments, in order to calculate post-extensional distances (supporting data shown on Table S2), which I plotted on Figure 3A in the main text.

For cross section 4, I utilized a reconstruction of extension across southeastern Idaho (~42-43° N latitude) from Rodgers et al. (2002; their Figure 4), which is supported by a series of range-scale cross sections that lie between 0 and 60 km along-strike to the north of the restored section line of cross section 4. The western edge of the deformed section of cross section 4 projects northward to the footwall of the normal fault bounding the east side of Gem Valley, which I used as a starting point on the Rodgers et al. (2002) reconstruction. The western edge of the restored section of cross section 4 projects to the Cassia Mountains, which lies near the western edge of the Rodgers et al. (2002) reconstruction. Cumulative extension values increase westward to 59.8 km, which is the sum of 11.1 km of extension along the deformed section of cross section 4 (Figure S1) and 48.7 km of extension on the Rodgers et al. (2002) reconstruction.

For cross section 5, I utilized the reconstruction of the Northern Basin and Range Province (~40° N latitude) from McQuarrie and Wernicke (2005; their Figure 3), which is supported by motion vectors compiled from published range-scale reconstructions that lie between 160-230 km along-strike to the south of the restored section line of cross section 5. The western edge of the deformed section line of cross section 5 projects southward to the western edge of the Canyon Range, and the western edge of the restored section line of cross section 5 projects southward to the western edge of the Northern Snake Range. The extension vectors in this region that I projected northward onto the restored section line of cross section 5 included the 40 km vector for the Cricket Range/Sevier Desert detachment, the 4 km vector for the House Range/"Reflection F" fault, the 4 km vector for the Confusion Range/House Range fault, and the 22 km (18-0 Ma) and 30 km (35-25 Ma) vectors for the Snake Range/Northern Snake Range décollement. Cumulative extension increases westward to 121.5 km, which is the sum of 21.5 km of total extension along the deformed section line of cross section 5 and 100 km of extension on the McQuarrie and Wernicke (2005) reconstruction.

For cross section 6, I utilized the reconstruction of Long (2019; his Plate DR1) at ~39° N latitude, which is supported by the deformed and restored versions of cross section 6 and a series of reconstructed range-scale cross sections that lie between 30 km along-strike to the south and 25 km along-strike to the north of the restored section line of cross section 6. The western edge of the restored section line of cross section 6 projects to the western edge of the Toiyabe Range on the restored cross section of Long (2019). Cumulative extension values increase westward to 152.9 km at the projected position of the Deep Creek Range (Figure S1).

For cross section 7, I utilized the reconstruction of the Central Basin and Range Province (~38° N latitude) from McQuarrie and Wernicke (2005; their Figure 4), which is supported by motion vectors from published reconstructions that lie between 20 km along-strike to the south and 25 km along-strike to the north of the restored section line for cross section 7. The western edge of the deformed cross section projects southward to the valley at the eastern edge of the Resting Spring range. The extension vectors that I projected onto the restored section line of cross section 7 included the two most proximal vectors, which are the 25 km vector from the Nopah/Resting Spring Range/Spring Mountains detachment and the 52 km vector from the Grapevine Mountains/Bare Mountain and Bullfrog detachments. Cumulative extension values increase northwestward to 80.6 km, which is the sum of 3.6 km of total extension along the deformed section line of cross section 7 (Figure S1) and 77 km of extension from the McQuarrie and Wernicke (2005) reconstruction.

Table S1 (see accompanying Excel table): Summary of parameters used to calculate shortening for the seven cross sections.

Table S2 (see accompanying Excel table): Summary table of: 1) distance measurements along the restored cross sections at which the cumulative thickness of pre-Cretaceous sedimentary rocks above the basal Sevier fold-thrust belt dècollement attained increments of 2.5 km; 2) incremental and cumulative extension values measured from the deformed cross sections and published reconstructions; and 3) accompanying post-extensional distances of the cumulative thicknesses of pre-Cretaceous sedimentary rocks (which are plotted on Figure 3A in the main text).

Table S3 (see accompanying Excel table): Summary of stratigraphic thickness measurements of rock units on the seven cross sections.

Table S4 (see accompanying Excel table): Supporting data for the graphs of thickening and thinning components shown on Figure 4B in the main text. See Figure 4A and section 4 in the main text for definitions of Z_{net}, Z_e, Z_{fb}, Z_{thr}, and Z_u. Z_u values for the region to the west of the deformed cross sections (i.e., west of 189 km on cross section 2 and west of 128 km on cross section 6) were measured using the difference in the depth to the Moho between the measured location and the western edge of the cross section. These Z_u values are likely minima, as the $^{87}Sr/^{86}Sr$ 0.706 isopleth lies between ~0-60 km to the west of the western edge of the restored sections (see section 5 in the main text for further discussion).

REFERENCES CITED

Christie-Blick, N., 1997, Neoproterozoic sedimentation and tectonics in west-central Utah, in Link, P.K., and Kowallis, B.J., eds., Proterozoic to recent stratigraphy, tectonics, and volcanology, Utah, Nevada, southern Idaho and central Mexico: Brigham Young University Geology Studies, v. 42, p. 1-30.

Coogan, J.C., 1992, Thrust systems and displacement transfer in the Wyoming-Idaho-Utah thrust belt [Ph.D. dissertation]: University of Wyoming, Laramie, Wyoming, 240 p., 55 figs., 2 plates.

DeCelles, P.G., 2004, Late Jurassic to Eocene evolution of the Cordilleran thrust belt and foreland basin system, western U.S.A.: American Journal of Science, v. 304, p. 105–168, doi: 10.2475/ajs.304.2.105.

DeCelles, P.G., and Coogan, J.C., 2006, Regional structure and kinematic history of the Sevier fold-and-thrust belt, Central Utah: Geological Society of America Bulletin, v. 118, p. 841-864, doi: 10.1130/B25759.1.

Fuentes, F., DeCelles, P.G., and Constenius, K.N., 2012, Regional structure and kinematic history of the Cordilleran fold-thrust belt in northwestern Montana, USA: Geosphere, v. 8, no. 5, p. 1104-1128, doi: 10.1130/GES00773.1.

Giallorenzo, M.A., Wells, M.L., Yonkee, W.A., Stockli, D.F., and Wernicke, B.P., 2018, Timing of exhumation of the Wheeler Pass thrust sheet, Southern Nevada and California: Late Jurassic to middle Cretaceous evolution of the Southern Sevier fold-and-thrust belt: Geological Society of America Bulletin, v. 130, no. 3-4, p. 558–579, doi: 10.1130/B31777.1.

Long, S.P., 2019, Geometry and magnitude of extension in the Basin and Range Province (39°N), California, Nevada, and Utah, U.S.A.: Constraints from a province-scale cross section: Geological Society of America Bulletin, v. 131, p. 99-119, doi: 10.1130/B31974.1.

McQuarrie, N., and Wernicke, B.P., 2005, An animated tectonic reconstruction of southwestern North America since 36 Ma: Geosphere, v. 1, p. 147–172, doi: 10.1130/GES00016.1.

Price, R.A., 1981, The Cordilleran foreland thrust and fold belt in the southern Canadian Rocky Mountains: Geological Society of London Special Publication 9, p. 427-448.

Rodgers, D.W., 1987, Thermal and structural evolution of the southern Deep Creek Range, west central Utah and east central Nevada [Ph.D. dissertation]: Palo Alto, California, Stanford University, 149 p., 5 plates.

Rodgers, D.W., Ore, H.T., Bobo, R.T., McQuarrie, N., and Zentner, N., 2002, Extension and subsidence of the Eastern Snake River Plain, Idaho, in Bonnichsen, B., White, C.M., and McCurry, M., Eds., Tectonic and Magmatic Evolution of the Snake River Plain Volcanic Province: Idaho Geological Survey Bulletin v. 30, p. 121-155.

Yonkee, W.A., Dehler, C.D., Link, P.K., Balgord, E.A., Keeley, J.A., Hayes, D.S., Wells, M.L., Fanning, C.M., and Johnston, S.M., 2014, Tectono-stratigraphic framework of Neoproterozoic to Cambrian strata, west-central U.S.: Protracted rifting, glaciation, and evolution of the North American Cordilleran margin: Earth-Science Reviews, v. 136, p. 59-95, doi: 10.1016/j.earscirev.2014.05.004.

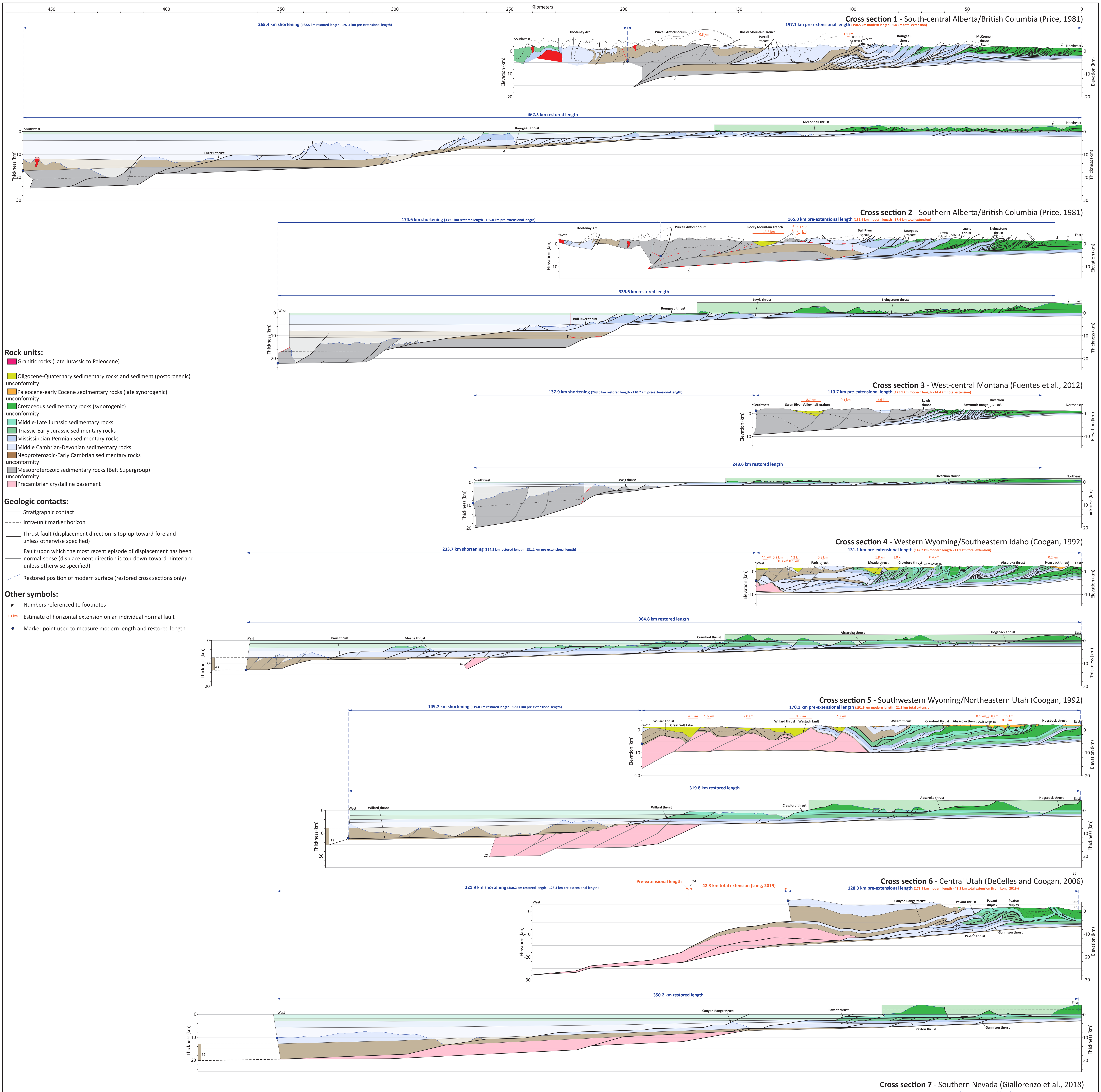

Footnotes:

1) For cross sections 1 and 2, the dark green 'Cretaceous sedimentary rocks' unit shown here includes the undifferentiated 'Upper Jurassic-Paleocene Foredeep Clastic Rocks' unit of Price (1981). The majority of this unit's thickness is Cretaceous in age, as the portion of this unit that could be as old as Late Jurassic (the Kootenay Formation) is less than 50 m thick in the foreland part of the cross section and is 300-400 m-thick in the westernmost preserved exposures (Price, 1981). The portion of this unit that could be as young as Paleocene is up to 600 m-thick in the foreland part of cross section 2.
2) The area of this thrust sheet that is here interpreted here as Belt Supergroup was left blank on Price (1981). Alternatively, this area could be filled by Precambrian basement.
3) The region of complexly folded rocks that lies to the southwest of this red line is not retro-deformed on the restored cross section.
4) The restored geometry shown to the southwest of this red line is from this study.
5) Cross section 2 lacks an emergent frontal thrust fault; therefore, I approximated the thrust front at the eastern limit of structural elevation in the Alberta Syncline.
6) The interpreted geometry for the region of cross section 2 that is outlined by this dashed red line is from this study, as it was left blank on Price (1981). I interpret this area as a single thrust sheet that carries a section of Belt Supergroup rocks, Neoproterozoic-Lower Cambrian rocks, and Middle Cambrian-Devonian rocks. The thickness shown for the Neoproterozoic-Lower Cambrian unit is the same as that shown in the hanging wall of the Purcell thrust on cross section 1, where it is constrained by surface exposures. The thickness shown for the Middle Cambrian-Devonian unit is based on the minimum exposed thickness in the hanging wall of the Bull River thrust.
7) The region of complexly folded rocks that lies below and to the west of this red line is not retro-deformed on the restored cross section.
8) The restored geometry shown below and to the west of this red line is from this study.
9) The restored geometry shown to the southwest of this red line is from this study.
10) The subsurface geometry of ramps through Precambrian crystalline basement rocks are unconstrained to the west of this point. It is possible that a flat dècollement extends westward of here, eventually meeting the dècollement at the base of the Neoproterozoic-Early Cambrian unit to the west, similar to the geometry shown by DeCelles and Coogan (2006).
11) In the Bannock Range, which is ~60 km along-strike to the north and ~25 km across-strike to the west of the western edge of this cross section (~15 km across-strike to the west after restoration of 10 km of extension; Rodgers et al., 2002), the basal dècollement underlies at least a 5.4 km cumulative thickness of Neoproterozoic-Early Cambrian sedimentary rocks (2.2 km of the Pocatello Formation (mininum), 2.1 km of the Brigham Group, and 1.1 km of Early Cambrian rocks; Yonkee et al., 2014).
12) The subsurface geometry of thrust faulting in Precambrian crystalline basement rocks is unconstrained to the west of this point. It is possible that a flat dècollement extends to the west of here, eventually meeting the dècollement at the base of the Neoproterozoic-Early Cambrian unit to the west, similar to the geometry shown by DeCelles and Coogan (2006).
13) In the Sheeprock Mountains, which are ~140 km along-strike to the south and up to ~10 km across-strike to the west of the western edge of this cross section, the basal dècollement underlies at least a 7.3 km cumulative thickness of Neoproterozoic-Early Cambrian rocks (3.2 km of the Sheeprock Group (minimum), 3.1 km of the Brigham Group, and 1.0 km of Early Cambrian rocks; Christie-Blick, 1997).
14) The deformed cross section of DeCelles and Coogan (2006) shown here is from their Figure 8F, which has been restored for 42.3 km of total Cenozoic extension (calculated using the reconstruction of Long, 2019). Readers are referred to Figure 3 of DeCelles and Coogan (2006) for a version of their deformed cross section that shows the present-day (i.e., post-extensional) geometry.
15) Cross section 6 lacks an emergent frontal thrust fault; therefore, I approximated the thrust front at the eastern limit of structural elevation in the frontal triangle zone.
16) In the Deep Creek Range, which is ~58 km along-strike to the north and ~39 km across-strike to the west of the western edge of this cross section (~33 km across-strike to the west when restored for 6 km of extension; Long, 2019), the basal decollement underlies at least a 7.3 km thickness of Neoproterozoic-Early Cambrian sedimentary rocks (3.6 km of the Trout Creek sequence (minimum), 2.4 km of the Brigham Group, and 1.3 km of Early Cambrian rocks; Rodgers, 1987).
17) The restored version of cross section 7 is from this study. The restored geometry was drafted to minimize displacement on thrust faults and thus minimize shortening. The Keystone thrust was restored so that its hanging wall ramp through the Bonanza King Formation lies just to the west of the western limit of the deformed cross section, which is the minimum displacement required based on the extent of the footwall flat in Upper Cambrian rocks (their unit Cu) shown on the deformed cross section. Based on this restoration, the combined minimum displacement on the Keystone thrust and its footwall imbricate (the Red Springs thrust) is 56 km. Paleozoic units thicken considerably westward between exposures in the footwall and hanging wall of the Keystone thrust. The Lee Canyon thrust was retro-deformed by restoring the hanging wall ramp through the Bonanza King Formation with its matching footwall ramp, which defines 11 km of displacement. The Wheeler Pass thrust was retro-deformed by restoring the hanging wall cutoff of the basal contact of the Bonanza King Formation with its matching footwall cutoff, which defines 16 km of displacement. The hanging wall ramp through units Zpm, Zj, Zs, and Zcw was used constrain the geometry of the corresponding footwall ramp in the westermost part of the restored section.